Journal of Applied Polymer Science

Mechanical Response of Poly(lactic acid)-Based Packaging Under Liquid Exposure

Indah Widiastuti, Igor Sbarski, Syed H. Masood
Swinburne University of Technology, Melbourne, Australia
Correspondence to: I. Widiastuti (E-mail: iwidiastuti@swin.edu.au or indahwied@yahoo.com)

ABSTRACT: The objective of this study was to examine the mechanical behavior of poly(lactic acid)-based packaging, which was subjected to an external load while undergoing dimensional and material property changes due to the diffusion of liquid through its thickness. We defined the characteristics of the material response by taking into account the changes in the properties due to liquid sorption. The material properties at any given location and time were dependent on the liquid content. In this article, we present the evolution of the mechanical behavior using a numerical stress model that accounts for the effects of the time, liquid content, temperature, and swelling-induced strain. We assumed that the deformation depended on the liquid concentration, but the liquid concentration could be obtained without the knowledge of the stress or strain. © 2014 Wiley Periodicals, Inc. J. Appl. Polym. Sci. **2014**, *131*, 40600.

KEYWORDS: biodegradable; degradation; packaging; swelling; theory and modeling

Received 1 December 2013; accepted 5 February 2014
DOI: 10.1002/app.40600

INTRODUCTION

Poly(lactic acid) (PLA)-based biodegradable polymers have been extensively used as commodity thermoplastics in packaging applications because of their good mechanical and optical properties; these include as a high stiffness, high technical strength, and transparency. Recent technologies have widened the processing capabilities in the production of not only flexible packaging but also of rigid containers for longer service life products, such as beverages (plain water, soft drink, and fruit juices), edible oil, and health and beauty products.[1] PLA-based materials, however, have some limitations as packaging materials, especially because of the deterioration of their material properties, which can observed after prolonged exposure to the environment.[2–4] Moreover, interactions involving the packaging type, product constituents, and environment may impact the material degradability and can initiate changes in the thermal, chemical, and physical properties of the material.

Numerous research works have reported reductions in the mechanical performance of PLA-based materials after the absorption of moisture under particularly humidity conditions.[4–8] Previous research has highlighted the significance of organic liquid absorption on the mechanical properties of PLA-based materials through the measurement of their static and dynamic properties.[9] The results show progressive decreases in the modulus and strength with increasing liquid content inside the material. The increase in the elongation was also observed; this indicated a plasticizing effect of liquid exposure on the PLA material. In packaging applications, the study of the sorption of a product constituent by the PLA package has attracted only a few studies to date. As majority of existing commercial applications are for food packaging, studies have mainly been focused on the barrier properties of food solutions related to the quality of the packaged product.[10–13] Recent reports on the interaction between PLA packaging and its product constituents have revealed changes in the thermomechanical properties after the sorption of a hydrophilic chemical compound into the package.[11,14,15] This finding highlighted sorption-induced plasticization in PLA packaging during its interaction with a particular substance of a packaged product.

The growing awareness of ecofriendly packaging has led to a rising demand for PLA packaging in a broader array of products. More semidurable and rigid packaging has been brought in and widely accepted into the market, not only for food-related products but also for consumer products. The discovery of new applications of PLA packaging for nonfood commodities and other products is a logical consequence of an increasing environmental awareness of the disposal of conventional plastic waste.

In the evaluation of new opportunities for PLA-based materials for chemical products or other aggressive liquid packaging, it is

Additional Supporting Information may be found in the online version of this article.

important to understand not only the chemical resistance of the material but also the potential routes for degradation.[16] In the mechanical behavior analysis of a package, it is also important to take into account the contribution of diffusion-induced swelling in the prediction of a more realistic stress state under loads. With the expectation of the use of a PLA-based material as an alternative for the application of chemical liquid packaging, a critical evaluation of the stress and deformation is needed to predict the reliability and failure behavior of such applications. Previous research has revealed the significance of the presence of a liquid on the relaxation process of the material.[9] The results show a decrease in the time-dependent modulus with increasing liquid content in the viscoelastic material; this accelerates with an increase in the environmental temperature.

The objective of this study was to numerically examine the mechanical behavior of PLA-based packaging, which was subjected to an external load while undergoing dimensional and material property changes due to the diffusion of liquid through its thickness. The study was designed to model reasonable worst case extraction when the polymer is used in commercial fluid container applications for intermediate time periods at various temperatures with an aggressive fluid simulant. This article presents the evolution of the mechanical behavior with a stress model that accounted for the effect of the time, liquid content, temperature, and swelling-induced strain. The effect of liquid diffusion was incorporated into the stress profile through the swelling coefficient (β) and liquid-dependent material parameters for both the elastic and transient (time-dependent) properties. We assumed that deformation depended on the liquid concentration, but the liquid concentration could be obtained without the knowledge of the stress or strain.

EXPERIMENTAL

The plastic material used in this study was a starch-based PLA resin produced by BIOTEC, a subsidiary company of Biome Technologies, which is known as Bioplast GS2189.[17] This compound polymer is composed of 90% corn-derived PLA and is reinforced with 10% potato starch.[18] The material, which was supplied in granule form, was converted into test samples according to the manufacturer's product manual with a Battenfeld BA 350/75 injection-molding machine.

The immersion fluid for this experiment was gasoline, which was provided by a local fuel station; it was composed of a 50/50 toluene–iso-octane mixture. For various levels of fluid concentration, different immersion temperatures were used to accelerate the level of liquid absorption. Unleaded gasoline was chosen because it was aggressive enough to accelerate the degradation that would occur in an application exposed to liquid and chemical solvents. Standard test method SAE J1748 was used in the immersion test. This method provides a standard for determining the physical properties of polymer materials exposed to a gasoline/oxygenated fuel mixture. The rectangular injection-molded samples were completely immersed in a hydrocarbon liquid in a ratio of three samples to 50 mL of liquid. The specimens were hanged with a stainless steel wire and separated with glass beads. The tubes were covered, and the samples were immersed to the point of saturation under four different conditions: (1) at room temperature, where the temperature was monitored with a digital thermometer at $20 \pm 3°C$; (2) in a fridge with the temperature monitored at $5 \pm 1°C$; and in a chamber set at (3) 30°C and (4) 50°C. Gravimetric measurement was used to determine the fluid uptake during the diffusion process. The specimens were removed periodically for weight measurement until saturation occurred. The determination of the saturated conditions was based on standard recommended by SAEJ1748,[19] in which we compared the data from two or more periods to determine that there was no significant difference among the period.

When the stress profile of the package was analyzed, the effect of the liquid diffusion was incorporated into the stress profile through β and the liquid-dependent material parameters for both the elastic and transient (time-dependent) properties. The constitutive model used to characterize the material was developed from a series of mechanical tests, in which we investigated changes in the material performance during the diffusion of the liquid. In evaluating the changes in mechanical properties with the amount of liquid absorption, mechanical tests were performed on saturated specimens to determine the properties at particular liquid contents. We did this to ensure that the mechanical properties were measured in specimens containing uniform liquid contents[20] and, thereby, to determine a more accurate relationship between the two parameters. Changes in the dynamic mechanical properties along with liquid content in the specimens were measured with a TA Instruments 2980 dynamic mechanical analyzer over the temperature range from 20 to 80°C at a frequency of 1 Hz. Creep experiments were also conducted in the same instrument used for dynamic mechanical analysis to obtain appropriate data for the modeling of the material viscoelastic properties. Samples with different levels of liquid content were clamped within the dynamic mechanical analyzer chamber in the film tensile creep mode. The experiment was undertaken at different isotherm temperatures to evaluate the influence of the temperature on the creep performances. For each isotherm, a constant stress of 0.45 MPa was applied for 60 min, and this was followed by a 10-min recovery period.

MODELING OF MATERIAL PROPERTIES

Because of the slow movement of liquid compared to the temperature, the material was submitted to nonuniform distribution over an extended period before it reached a saturated condition.[21] Initially, a higher liquid concentration was present near the surface at which the absorption occurred more rapidly rather than in the inner layers, and then, the material moved toward equilibrium liquid concentration as time passed. As a result, the property changes associated with the presence of the liquid were not uniformly distributed within the material.[22] The variation in the material properties during diffusion was represented by dependency of the modulus on the liquid content and was a function of the position and the time. The responses of the material in contact with the liquid environment were characterized through a constitutive model, which accounted for

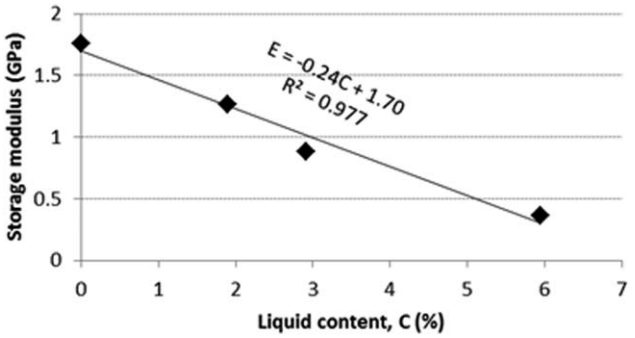

Figure 1. Linear relationship of the storage modulus (E) and the liquid content (C) where the strength of linear relation is indicated from the value of R^2. The elastic modulus of the dry material was equal to 1.7 GPa.

changes in the modulus of the material. For simplification, in this case, we assumed that Poisson's ratio remained constant and was independent of the liquid content.

The definition of the material in the finite element (FE) model was specified from the experimental data, as given in Section 2. The function of the modulus with liquid content was obtained from the result of the storage modulus, as presented in Figure 1. The results presented in Figure 1 were obtained from the dynamic property measurement, as explained previously in the Experimental section.

A viscoelastic model with a mechanical analogy model with a four-element Burger model was applied to represent the creep behavior of the PLA-based material subjected to liquid diffusion. The creep strain defined by the time-dependent constitutive equation for constant stress, which consisted of elastic and viscous deformation, could be represented by Burger's model[23–27] as follows:

$$\varepsilon(t)=\sigma\left\{\frac{1}{E_M}+\frac{1}{E_K}\left[1-\exp\left(-t\frac{E_K}{\eta_K}\right)\right]+\frac{t}{\eta_M}\right\} \quad (1)$$

Because of the effect of the liquid content inside the material, a modified Burger's model from eq. (1) was developed to analytically represent the relationship between the creep parameters and the liquid content at a specified temperature. The creep strain was given by the following equation:

$$\varepsilon(t)=\frac{\sigma}{f_{E_M}(C)}+\frac{\sigma}{f_{E_K}(C)}\left[1-\exp\left(-t\frac{E_K}{\eta_K}\right)\right]+\frac{\sigma}{f_{\eta_M}(C)}t \quad (2)$$

where $\varepsilon(t)$ is the time-dependent strain, σ is the applied stress, and t is the time. In this model, the functions f_{EM}, f_{EK}, f_τ, and $f_{\eta M}$ represent changes in the creep parameter as a function of the liquid content at a given temperature. E_M and E_K are the elastic moduli of the Maxwell and Kelvin springs, respectively, and η_M and η_K are the viscosities of the Maxwell and Kelvin dashpots, respectively. This model has one retardation time, $\tau = E_K/\eta_K$. One can obtain the parameters in eq. (2) by fitting the equation to the experimental data.

In defining the time-dependent properties of a material in the computational program, the material is described as having an initial linear isotropic response to the load and thereafter as having an ability to creep with time hardening over primary and secondary phases. Recommended as the most accurate means to represent the creep, the implicit model was used to simulate the creep stages in ANSYS software.[28,29] In this case, the combined time-hardening creep model, which was used to directly model the primary and secondary creep effects, was chosen to simulate the material response. The creep strain (ε_{cr}) over time could be described as follows:[30]

$$\varepsilon_{cr}=\left[\frac{C_1\sigma^{C_2}t^{C_3+1}e^{\frac{-C_4}{C(t)}}}{(C_3+1)}\right]+\left[C_5\sigma^{C_6}te^{\frac{-C_7}{C(t)}}\right] \quad (3)$$

where C_i is the coefficient derived by the FE software and $C(t)$ is the liquid content at time t. The results of the ANSYS nonlinear curve regression were verified by insertion of the generated coefficients into eq. (3). The curve-fitting procedure was then applied for the material containing different concentrations of liquid, and this resulted in the creep model coefficients C_1–C_7, as given in Table I.

The coefficients given in Table I were implemented by the incorporation of the instantaneous elastic response in the analysis. Table I shows the effects of the liquid content on the coefficients of the creep equation at particular temperatures. The effect of the environmental temperature on the creep coefficients in eq. (3) is shown in Figure 2. In this figure

$$\Delta T=(T-T_0)/T_0$$

where T_0 is defined as equal to 30°C and T is the specified environmental temperature, while ΔT indicates the temperature difference.

The numerical ANSYS results of the elastic and creep strains were plotted against the observed experimental results, and the analytical model, as presented in eq. (2), is shown in Figure 3.

As shown in Figure 3, the creep strain curve generated by the numerical model for the dry PLA-based material showed a good correlation with the experimental results and the analytical model shown in eq. (2).

RESULTS AND DISCUSSION

The stress associated with a diffused liquid can be analyzed with the general technique of thermal stress analogy because liquid diffusion is mathematically equivalent to the heat-transfer process.[31] However, for complicated problems in which it might be difficult to obtain an exact closed-form analytical solution, the FE method is often used to find an approximate solution.[32] A numerical analysis based on the FE approach was proposed here to study the coupled diffusion and stress in the packaging application. To ensure that the FE model accurately predicted the mechanical response of the application, it was imperative to examine some factors that may have affected the accuracy of the obtained results. We carried out the convergence study by comparing the field responses from the FE analysis with the analytical solution of the simplified version of the problem, as described in the Supporting Information. The analytical and numerical solutions with the FEA (Finite Element Analysis) method agreed well.

Mechanical Response of a Packaging Application

In developmental phase of a new package design, performance tests are usually performed before the package is qualified for packaging applications; these include the analysis of its permeability to liquid and gas, environmental stress cracking

Table I. Creep Model Coefficients for the PLA-Based Materials Containing Various Levels of Liquid at 30°C

	Coefficients for the implicit creep equation [eq. (2)]						
Liquid content (%)	C_1	C_2	C_3	C_4	C_5	C_6	C_7
0	6.20×10^{-6}	1.35×10^{-9}	−0.566	0	7.84×10^{-8}	6.02×10^{-10}	0
1.90	2.24×10^{-5}	1.04×10^{-8}	−0.542	0	3.46×10^{-7}	3.81×10^{-7}	0
2.91	3.64×10^{-5}	8.16×10^{-8}	−0.583	0	2.58×10^{-7}	-2.38×10^{-8}	0
5.95	1.57×10^{-4}	9.28×10^{-8}	−0.882	0	1.50×10^{-7}	-6.14×10^{-9}	0

resistance, and crystallinity and structural tests.[33] Structural analysis in packaging applications is done to verify the mechanical strength of the package and identify key areas of structural weakness in relation to the design and thickness distribution of the package.[34,35] Mechanical performance tests commonly conducted are the burst pressure test, top-load analysis, and drop test. To evaluate the durability of the package during its life service, the strength of application is assessed by the measurement of the package's stress and deformation in response to various loads.[36] Usually, this is followed by analysis of the critical load at the point of buckling, or the *buckling load*.[37] The FE method has been implemented in numerous studies to assess the structural performance of various package designs subjected to different loading conditions.[33,37–40] Those studies confirmed the advantages of FE analysis in the evaluation of the mechanical performance of a package in its early phase of design. Simulation-driven product development supplements expensive experimental costs and complex testing in packaging applications.[41]

To investigate the effect of liquid transport on the mechanical performance of a packaging application, we implemented a mechanical behavior study for a general small-size package with a thickness of 1 mm by means of the FE model and focused on top-load and internal pressure analysis. FE analysis was performed with the converged mesh and time-step sizes evaluated previously in the convergence analysis for a small container, as shown in Figure 4.

As the purpose of this study was to evaluate the significance of the diffusion in relation to the mechanical response, the simulation was concentrated on the region of the package base, which was constantly in contact with the diffusant. In the simulation stage, the boundary conditions were defined in the FE software according to the conditions that the package experienced while in service during storage after filling. For the structural analysis of the package, instead of using a constant value to define the material properties, we used liquid-content-dependent mechanical properties, especially for the modulus. The material properties required for stress and deformation analysis were defined on the basis of the coefficients of the creep equation given in Table I, which represented the viscoelastic properties of the material.

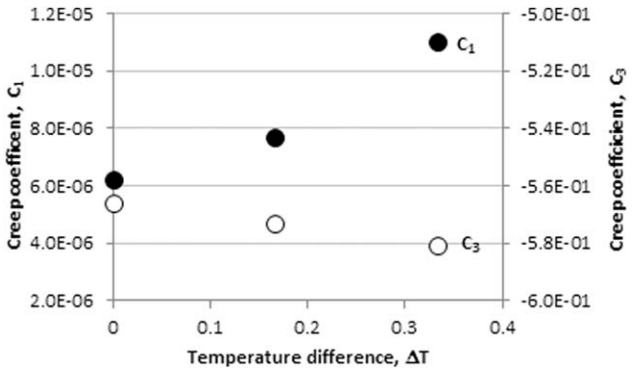

Figure 2. Effects of the environmental temperature on C_1 and C_3 from eq. (2).

Profile of the Liquid Content. The distribution of the liquid content within the thickness of the package was first determined with the transient heat-transfer module in the FE software. Characteristics of the liquid diffusion into the PLA package are described in Table II.

Using the value of the diffusion coefficient (D) provided in Table II, we obtained the profile of liquid content in the packaging at a 20°C environmental temperature at time t, as shown in Figure 5 for $t = 550$ h.

The simulation result in Figure 5 presents a nonuniform distribution of liquid concentration before saturation conditions with the minimum concentration occurring on the fillet section of the package base. The evolution of the liquid content was then transferred into the static structural section of the FE software to investigate the mechanical responses of the various loading conditions applied.

Top-Load Analysis. In this analysis, the performance of a liquid container made of a PLA-based plastic containing a hydrocarbon liquid was evaluated by the simulation of the mechanical behavior under a top load by means of the FE model. The top-

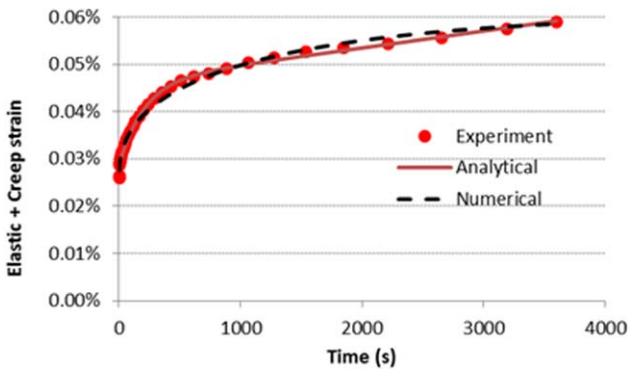

Figure 3. Numerical results versus experimental results for the elastic and creep strains in the dry material conditioned at 30°C. [Color figure can be viewed in the online issue, which is available at wileyonlinelibrary.com.]

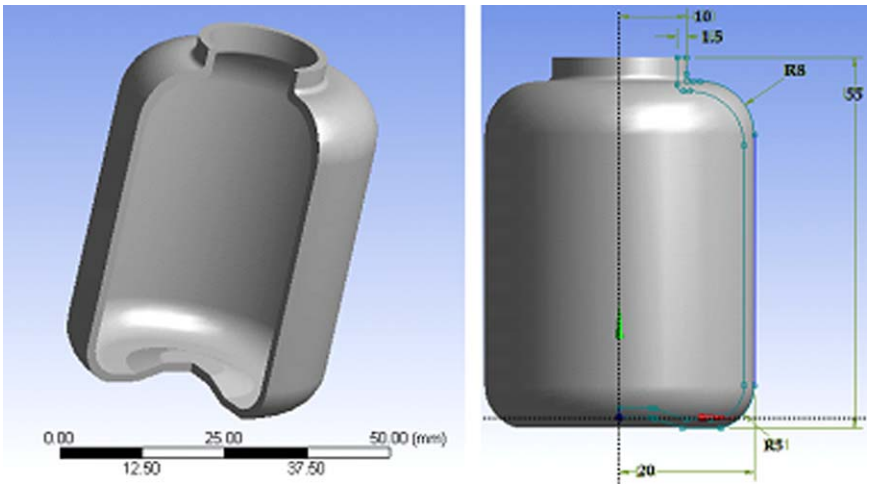

Figure 4. Design of the simulated liquid package with the corresponding dimensions (in millimeters). [Color figure can be viewed in the online issue, which is available at wileyonlinelibrary.com.]

load analysis aims to assess the durability of packages to withstand the axial load necessary to fill and stack the packages during manufacturing, storage, and distribution.[36,41] The top-load test is usually performed to identify the peak buckling load, which is the critical load that results in buckling. The response to the applied load is initially linear, but at a certain point, the compression force no longer increases linearly with applied deformation.[37] This is the critical point where buckling starts. The boundary conditions for the top-load analysis are as shown in Figure 6.

The equivalent (von Mises) stress and deformation profiles of the package resulting from FE software are shown in Figure 7. The von Mises stress was maximum at the bottom part of the package base, which was related to the constrained location, where the bottle rests.[34]

In the package wall, the tangential stress concentration was at the outer surface, as shown in Figure 8, because of the inhomogeneous liquid content, which resulted in swelling-induced stress. This critical stress point may become an indication for the possibility of failure in a package. When the resulting stress exceeds the yield stress of the package material, stress cracking may occur, especially with the presence of high deformation.[42]

The mechanical responses of the packages with different wall thicknesses exposed to different levels of environmental temperatures were obtained by the application of a dimensionless variable of Fourier number (F_0) as a function of diffusion coefficient D, time t and the thickness d; which can be calculated with the following equation:[43,44]

Table II. Characteristics of Liquid Diffusion at Various Environmental Temperatures

	5°C	20°C	30°C
D (m^2/s)	0.57×10^{-12}	1.10×10^{-12}	1.13×10^{-12}
C_m (%)	1.90	2.91	5.95
B	3.32×10^{-2}	5.31×10^{-2}	9.92×10^{-2}

$$F_0 = \frac{Dt}{\delta^2} \quad (4)$$

Equation (4) indicates that at the same value of time, if the value of the wall thickness is larger, the value of F_0 will be lower.

The effect of the degradation rate, β, and the environmental temperature on the mechanical response is discussed in the following subsections. Because the peak load capacity of a package is influenced by the nonlinear material properties,[45] the effect of those parameters on the buckling load were also evaluated.

Effect of the degradation rate. The effects of the rate of liquid-diffusion-induced degradation on the stress and deformation fields were studied. In the elastic approach, the degradation rate is determined from the slope of the decreasing line of the modulus with liquid concentration. According to the experimental results, as presented in Figure 1, the degradation rate of the elastic modulus was obtained from the gradient of the regression function, which was equal to 0.24. For comparison, another case with no degradation, a dry material with a constant modulus, was considered.

Figure 9 portrays the evolution of the total radial deflection and stresses at the package wall for the two different degradation rates. Figure 9(a) shows that the applied load to the material, which experienced degradation in its modulus, resulted in a higher deflection compared to that which did not consider the deterioration of the material properties. However, deformation was still been apparent for the case of constant modulus because of the diffusion-induced swelling effect. Loss of the package integrity could occur with high undesirable deformations; this resulted from the material property deterioration induced by liquid diffusion. In terms of stress fields, the evolution of equivalent (von Mises) stress and tangential stress at the package wall with time were obvious as a result of nonuniform expansion before saturated conditions were reached. Figure 9(b,c) shows that the peak of stress was observed at a value of F_0 of about 0.2. As a result of the lower modulus, lesser values of stresses for the material, which experienced a degraded

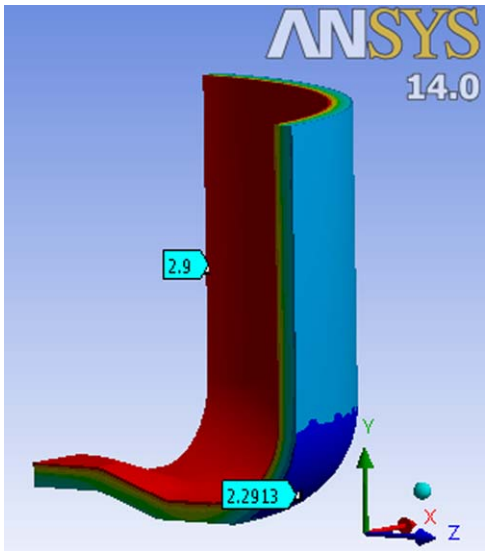

Figure 5. Profile of the liquid content within the thickness of the package base at $t = 550$ h. [Color figure can be viewed in the online issue, which is available at wileyonlinelibrary.com.]

modulus, were revealed, especially in the early period of the diffusion process.

Buckling analysis was performed after the structural analysis to identify the changes in buckling strength with the rate of degradation. The result of linear buckling analysis generated from the FE software is presented in Figure 10. The result indicates that the buckling strength fell from 190.3 MPa for the material with no degradation to 103.5 MPa for the material with a 0.24 degradation rate. A decrease in the top-load strength was also observed by Abbès et al.[39] in the case of increasing ethyl acetate concentration in polypropylene bottles.

Effects of the time-dependent properties. The effects of time-dependent values on the material constitutive equation were investigated by the simulation of two different cases (cases 1

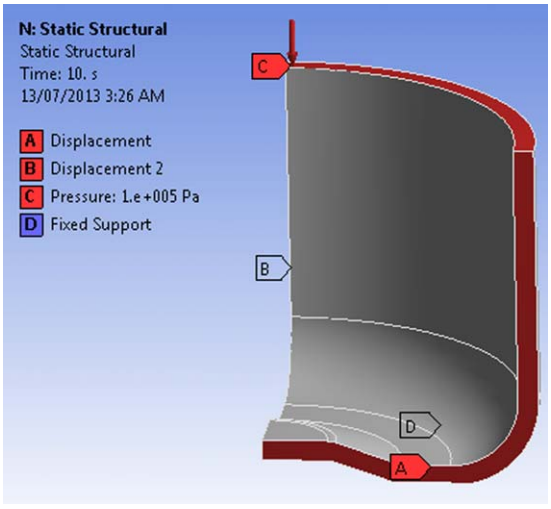

Figure 6. Boundary conditions for the top-load analysis of the package base. [Color figure can be viewed in the online issue, which is available at wileyonlinelibrary.com.]

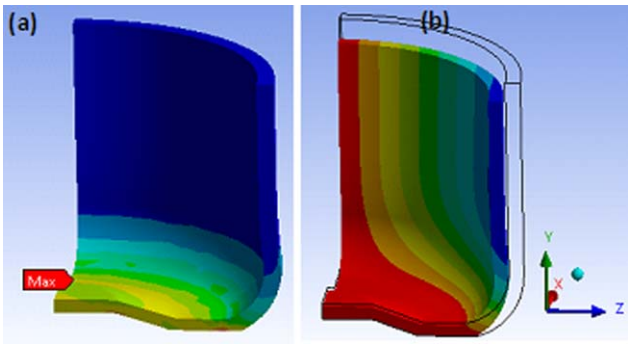

Figure 7. Distribution of (a) the von Mises stress and (b) the radial deflection of the package under top loading. [Color figure can be viewed in the online issue, which is available at wileyonlinelibrary.com.]

and 2) with different creep parameters. These two cases were simulated with the coefficients of the creep equation presented in Table I. For case 1, the material properties were modeled with the creep model in eq. (3) with the coefficients of the dry material (0% liquid concentration). In case 2, the material properties were modeled with liquid-content-dependent creep coefficients instead of constant coefficients by the modification of eq. (3) as follows:

$$\varepsilon_{cr} = \left(\frac{C_1[C(t)]\sigma^{C_2[C(t)]} t^{C_3[C(t)]+1}}{\{C_3[C(t)]+1\}} \right) + \left\{ C_5[C(t)]\sigma^{C_6[C(t)]} t \right\} \quad (5)$$

where C_i is the coefficient of the creep equation, which was obtained empirically from the data presented in Table I.

The deformation and stress fields for those two cases are shown in Figure 11. For comparison, another case of time-independent properties is also presented. The deflection of the material calculated with both the elastic and viscoelastic approaches increased significantly with time as a result of time-dependent diffusion-induced swelling. The higher deflection in the viscoelastic material was pronounced, especially when the viscoelastic material properties degraded with liquid content, as in case 2. The evolution of the tangential stress with time was also observed; it peaked at the same value of F_0, around 0.2. Figure 11(b) shows

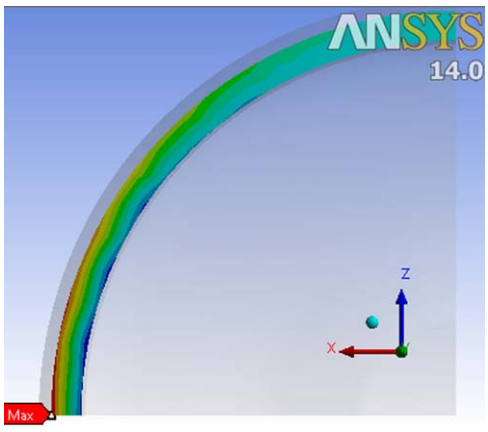

Figure 8. Critical tangential stress areas at the outer surface of the package wall under top loading. [Color figure can be viewed in the online issue, which is available at wileyonlinelibrary.com.]

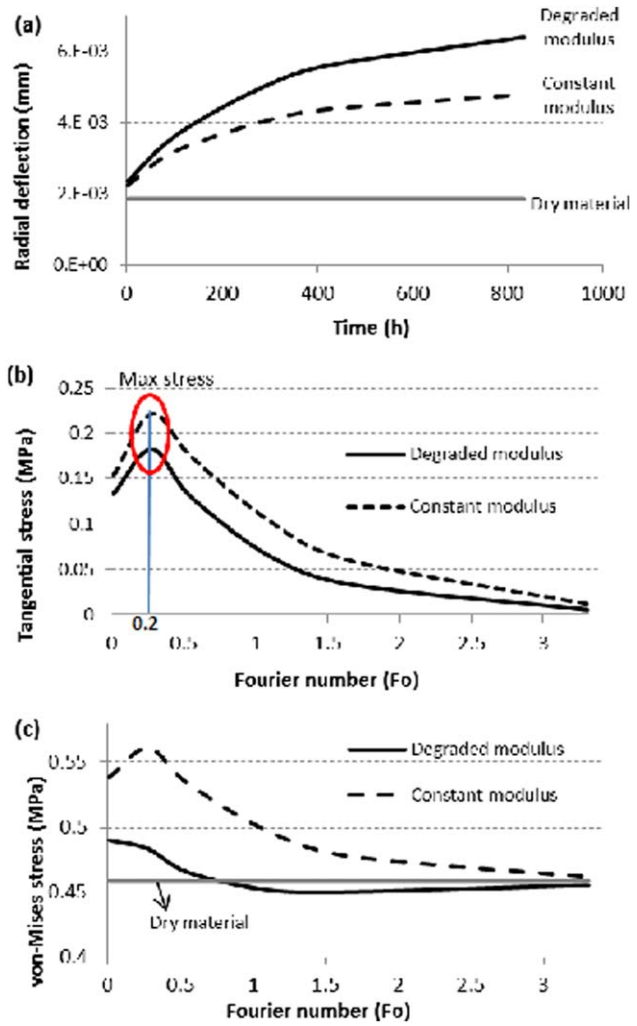

Figure 9. Evolution of the mechanical responses of an elastic package at different rates of degradation to the (a) radial deflection, (b) tangential stress at the package wall, and (c) von Mises stress. [Color figure can be viewed in the online issue, which is available at wileyonlinelibrary.com.]

that the elastic solution gave an overestimation of the stress component, but the curves coincided with the viscoelastic solution after the saturated liquid concentration (C_m) was achieved in the material. In the viscoelastic material, the increase of the time-dependent modulus with increasing liquid content led to a higher deformation compared to that in the elastic material.

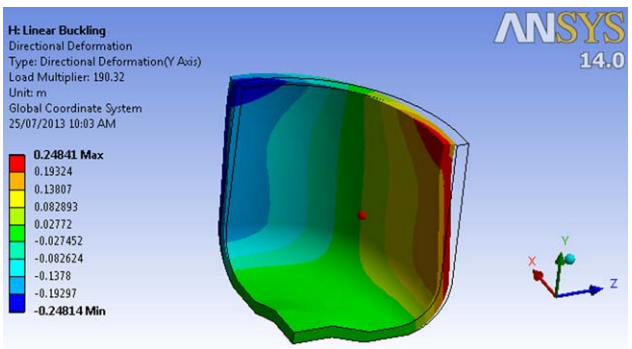

Figure 10. Simulated buckling in the PLA-based package under a top load. [Color figure can be viewed in the online issue, which is available at wileyonlinelibrary.com.]

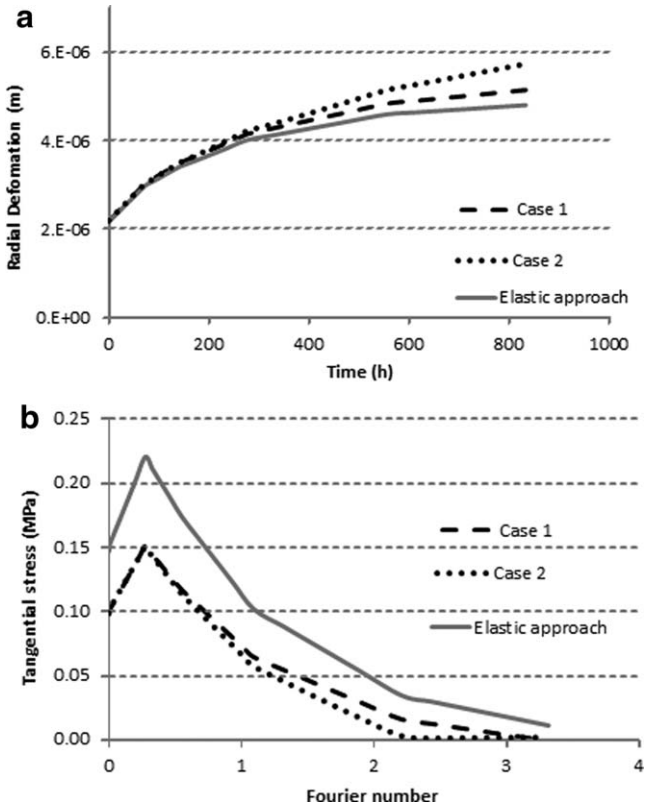

Figure 11. Evolution of the mechanical responses of a viscoelastic package for different liquid dependences of the creep parameters on the (a) radial deflection and (b) tangential stress at the package wall.

Effect of the environmental temperature. The effect of the environmental temperature on the mechanical response of the package with the presence of liquid was also analyzed. Simulation was performed with the data of the liquid diffusion characteristics for different environmental temperatures, as shown in Table II and the creep parameters obtained from the tabulation of the experimental data presented previously in Figure 2.

Significant effects of the environmental temperature on the strain and stress states of the package are clearly shown in Figure 12. It is shown in this figure that the peak of stress at all environmental temperature occurred at the same value of F_0 of 0.2. The figure also displays the increase in the stress with an increase in temperature. The higher the environmental temperature was, the higher the deflection and tangential stresses were. As shown in Figure 12(b), the tangential stress at the package wall increased with increasing environmental temperature; this potentially weakened the sidewall panel of the package.[16,46] This phenomenon was due to the high β and high creep coefficients at elevated temperatures.

Internal Pressure Analysis. The mechanical performance of a package can also be assessed through a burst strength analysis, which evaluates the stability of a package subjected to an internal pressure. This test is usually performed for bottles intended for carbonated beverages to ensure that the bottles do not blow up at the filling stage and that filled bottles do not expand

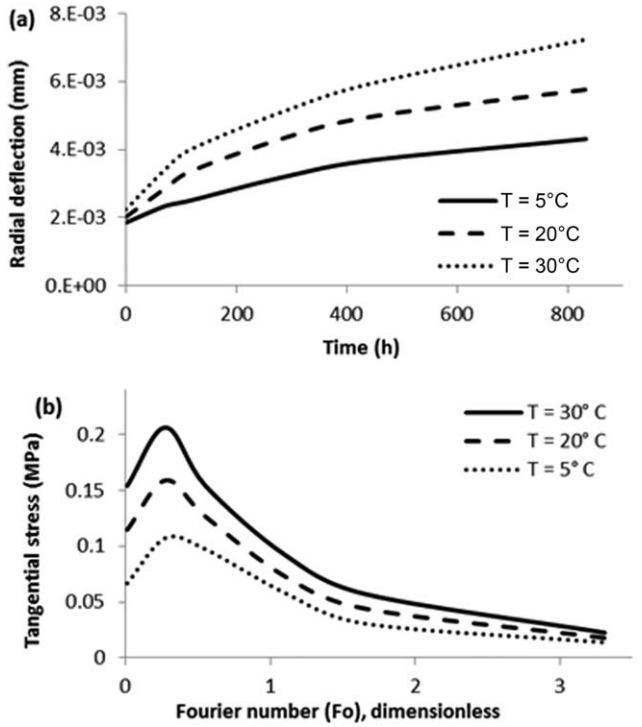

Figure 12. Evolution of the mechanical responses of an elastic package under different environmental temperature conditions to the (a) radial deflection and (b) tangential stress at the package wall.

excessively during storage and/or bottle warming for pasteurization purposes.[36] When internal pressure analysis is done with the FE model, the top section of the bottle is clamped, and an internal pressure is applied to the inner surface. The test result provides an assessment of the overall stability of the bottle under the carbonation pressure of the contents and establishes qualitative and quantitative statements on the widening of the package. In addition to the internal pressure analysis, a similar test with a vacuum pressure could also be performed to assess the vacuum resistance of the package.[37] A phenomenon called *paneling* can be observed when the internal stress under pressure exceeds the vacuum resistance.

In applications of PLA material for liquid packaging, it has been found that inward deformation or paneling occurs in the container after storage for a particular period of time.[47,48] Inward buckling takes place in the package because of a pressure difference with the ambient air pressure outside.[49] The permeation of gas/water vapor creates a negative pressure and causes the walls of the package to be sucked in to compensate for the loss of volume.

To illustrate the phenomenon of paneling due to gas/water vapor permeation, we proposed an FEA model to predict the critical period, which corresponded to the inward buckling point. The critical buckling load was obtained first in a static structural model of the FE software on the basis of specified loading and boundary conditions. The estimated critical load was then correlated to the radial stress at the internal package wall in response to the package shrinkage due to permeation. The critical buckling load in part of a package subjected to an

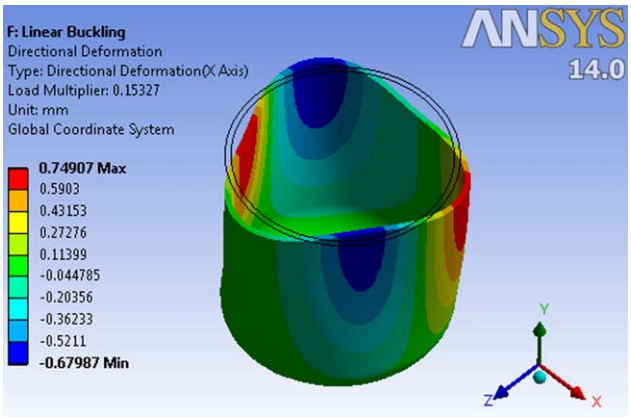

Figure 13. Buckling of the package in response to the internal vacuum pressure. [Color figure can be viewed in the online issue, which is available at wileyonlinelibrary.com.]

internal vacuum pressure is presented in Figure 13, which shows a value of 0.153 MPa.

Another FEA model was developed to simulate the process of substance permeation through the package, as shown in Figure 14. The static structure module was then added to the model to determine the stress induced in the package. The maximum axial stress in the x direction in the package wall is shown in Figure 15. Figure 15 shows the increasing trend of axial stress during the storage period due to water and hydrocarbon loss through the package wall. Inward buckling occurred at a time when the axial stress exceeded the specified buckling limit of 0.153 MPa. As shown in Figure 15, the buckling of the package containing water and hydrocarbon occurred at t values of 110 and 60 days.

CONCLUSIONS

In this article, we present the response of a PLA-based package in contact with liquid and subjected to mechanical loading with an FE model. The effect of the time-varying liquid content was examined in terms of the stress and deformation fields. The model was developed according to a series of convergence analyses to ensure that the results obtained were adequately accurate. We found that the size of the time increment significantly affected the accuracy of the results.

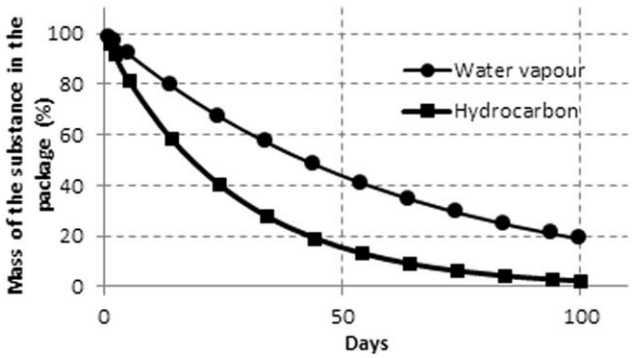

Figure 14. Simulation results for the loss of water and hydrocarbon substance in a PLA package with a 1-mm thickness at room temperature.

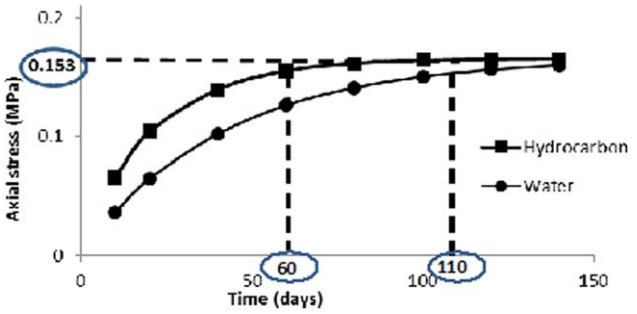

Figure 15. Evolution of the axial stress resulting from water and hydrocarbon loss through the wall of a package. [Color figure can be viewed in the online issue, which is available at wileyonlinelibrary.com.]

A viscoelastic model was developed in the FE software with creep implicit schemes to represent the time-dependent properties of the material. As it was to be expected, a higher temperature accelerated more relaxation in the material; this increased the deformation. The resulting stress increased with increasing temperature because the time-dependent modulus and β were dependent on the temperature.

The package was subjected to a uniform load at the top of the package, and the effects of the degradation rate and β were investigated. The stress concentration arose at the outer surface at the wall as a result of different expansion due to nonuniform liquid contents. The variation of swelling acted as an internal constraint, as it induced stresses that were developed during the liquid diffusion process. The combination of the mechanical and swelling stresses became exceptionally large; this reduced the load-bearing capacity and resulted in crack initiation, which led to failure of the application. The result confirmed the substantial influence of β, which showed a higher stress with increasing β. For packaging applications, serious consideration must be given to the degradation of the material properties after the sorption of a product substance into the package. A higher degradation rate with liquid content may result in the loss of the package integrity because of high undesirable deformations occurring in the package.

ACKNOWLEDGMENTS

One of the authors (I.W.) thanks the Indonesian Directorate General of Higher Education for a fellowship.

REFERENCES

1. NatureWorks. *Technical data sheet: Ingeo™ Biopolymer 7001D*: [Online]. NatureWorks LLC. [Accessed on April 2012].
2. Sharp, J. S.; Forrest, J. A.; Jones, R. A. L. *Macromolecules* **2001**, *34*, 8752.
3. Van Aardt, M.; Duncan, S. E.; Marcy, J. E.; Long, T. E.; O'Keefe, S. F.; Sims, S. R. *Int. J. Food Sci. Technol.* **2007**, *42*, 1327.
4. Holm, V. K.; Ndoni, S.; Risbo, J. *J. Food Sci.* **2006**, *71*, E40.
5. Ho, K. L. G.; Pometto, A. L., III; Hinz, P. N. *J. Environ. Polym. Degrad.* **1999**, *7*, 83.
6. Copinet, A.; Bertrand, C.; Govindin, S.; Coma, V.; Couturier, Y. *Chemosphere* **2004**, *55*, 763.
7. Harris, A. M.; Lee, E. C. *J. Appl. Polym. Sci.* **2010**, *115*, 1380.
8. Niaounakis, M.; Kontou, E.; Xanthis, M. *J. Appl. Polym. Sci.* **2011**, *119*, 472.
9. Widiastuti, I.; Sbarski, I.; Masood, S. H. *J. Appl. Polym. Sci.* **2013**, *127*, 2654.
10. Auras, R.; Singh, S. P.; Singh, J. *J. Test. Eval.* **2006**, *34*, 530.
11. Colomines, G.; Ducruet, V.; Courgneau, Ć.; Guinault, A.; Domenek, S. *Polym. Int.* **2010**, *59*, 818.
12. Haugaard, V. K.; Weber, C. J.; Danielsen, R.; Bertelsen, G. *Eur. Food Res. Technol.* **2002**, *214*, 423.
13. Dmytrów, I.; Szczepanik, G.; Kryza, K.; Mituniewicz-Małek, A.; Lisiecki, S. *Int. J. Dairy Technol.* **2011**, *64*, 569.
14. Salazar, R.; Domenek, S.; Courgneau, C.; Ducruet, V. *Polym. Degrad. Stab.* **2012**, *97*, 1871.
15. Courgneau, C.; Domenek, S.; Lebossé, R.; Guinault, A.; Avérous, L.; Ducruet, V. *Polym. Int.* **2012**, *61*, 180.
16. Duncan, B.; Urquhart, J.; Roberts, S. Review of Measurement and Modelling of Permeation and Diffusion in Polymers. Hampton Road, Teddington, Middlesex, UK: National Physical Laboratory. **2005**.
17. Biotec. *Technical Information: Bioplast GS2189* [Online]. Biotec. Available: http://www.biotec.de/engl/products/bioplast%20gs2189_engl.pdf. [Accessed on December 2010]
18. Almeida, D. N. F. D. Mechanical Engineering; Instituto Superior Tecnico Universidade Tecnica de Lisboa: Lisbon, **2011**.
19. SAE J1748: SAE Handbook; Society of Automotive Engineers: Warrendale, PA, 2005.
20. Jia, N.; Fraenkel, H. A.; Kagan, V. A. *J. Reinforced Plast. Compos.* **2004**, *23*, 729.
21. Tounsi, A.; Adda-Bedia, E.; Serei, Z.; Benhassaïni, H. *Arab. J. Sci. Eng.* **2003**, *28*, 23.
22. Paterson, M. W. A.; White, J. R. *J. Mater. Sci.* **1992**, *27*, 6229.
23. Nunez, A. J.; Marcovich, N. E.; Aranguren, M. I. *Polym. Eng. Sci.* **2004**, *44*, 1594.
24. Xu, Y.; Wu, Q.; Lei, Y.; Yao, F. *Bioresour. Technol.* **2010**, *101*, 3280.
25. Tang, X. G.; Hou, M.; Zou, J.; Truss, R.; Zhu, Z. *Compos. Sci. Technol.* **2012**, *72*, 1656.
26. Ludueña, L.; Vázquez, A.; Alvarez, V. *J. Compos. Mater.* **2012**, *46*, 677.
27. Pérez, C. J.; Alvarez, V. A.; Vázquez, A. *Mater. Sci. Eng. A* **2008**, *480*, 259.
28. Dropik, M. J.; Johnson, D. H.; Roth, D. E. Presented at International ANSYS Conference and Exposition, Pittsburgh, PA, April **2002**.
29. Gimbert, S. Architectural Engineering; Pennsylvania State University: Philadelphia, **2008**.
30. ANSYS, Inc. Verification Manual for the Mechanical APDL Application. **2009**.

31. Huang, M.; Thompson, V. P.; Rekow, E. D.; Soboyejo, W. O. *J. Biomed. Mater. Res. B* **2008**, *84*, 124.
32. Shah, S.; Muliana, A.; Rajagopal, K. R. *Mech. Time-Dependent Mater.* **2009**, *13*, 121.
33. Demirel, B. *Optimisation of Petaloid Base Dimensions and Process Operating Conditions to Minimise Environmental Stress Cracking In Injection Stretch Blow Moulded PET Bottles* Doctor of Philosophy, RMIT University. **2008**.
34. Erbulut, D. U.; Vasa, S.; Masood, S. H.; Davies, K. 2009 Annual Technical Conference; Chicago, **2009**; p 55.
35. Haddad, H.; Masood, S.; Erbulut, D. U. *Aust. J. Mech. Eng.* **2009**, *7*, 69.
36. Demirel, B.; Daver, F. *J. Appl. Polym. Sci.* **2012**, *126*, 1300.
37. Van Dijk, R.; Sterk, J. C.; Sgorbani, D.; Van Keulen, F. *Packaging Technol. Sci.* **1998**, *11*, 91.
38. Vaidya, R. *Structural Analysis of Poly Ethylene Terephthalate Bottles Using Finite Element Method.* Master of Science, Oklahoma State University. **2012**.
39. Abbès, B.; Zaki, O.; Safa, L. *Polym. Test* **2010**, *29*, 902.
40. Masood, S. H.; Satyanarayana, V.; Erbulut, U. Design and development of large collapsible PET water cooler bottles. International Conference on Computer Graphics, Imaging and Visualisation, 26–28 July 2006, **2006** Sydney; Australia. 528–533.
41. Robertson, N.; Metwally, H. Virtual prototyping in the manufacture and design of plastic packaging. ANSYS, Inc. **2013**.
42. Miranda, C. A. S. D.; Câmara, J. J. D.; Monken, O. P.; Santos, C. G. D. *J. Mater. Sci. Eng. B* **2011**, *1*, 947.
43. Carslaw, H. S.; Jaeger, J. C. Conduction of Heat in Solids; Oxford University Press: New York, **1986**.
44. Crank, J. The Mathematics of Diffusion; Oxford University Press: Oxford, United Kingdom, **1967**.
45. McNabb, R.; Kemp, M.; McMahon, S. *An Advanced Method for Optimizing Packaging Design* [Online]. Altair Engineering Ltd, **2002**. [Accessed June 2013].
46. NatureWorks. *Evaluation of Jojoba Oil in Ingeo Bottles* [Online]. NatureWorks LLC. **2011**. Available: http://www.natureworksllc.com/~/media/Technical_Resources/Fact_Sheets/FactSheet_Evaluation-of-Jojobo-Oil-in-Ingeo-Bottles_pdf.pdf. Accessed on February 2012.
47. Singh, V. M. Chemical Engineering; Drexel University: Philadelphia, **2008**.
48. Cairncross, R. A.; Becker, J. G.; Ramaswamy, S.; O'Connor, R. *Appl. Biochem. Biotechnol.* **2006**, *131*, 774.
49. O. Berk, *Plastic Bottle Paneling: 5 Causes and The Cures* [Online]. New Jersey, USA: O. Berk. **2012**. [Accessed on June 2013].